Biomass Conversion and Biorefinery
https://doi.org/10.1007/s13399-024-05937-z

ORIGINAL ARTICLE

Characterization of fly ash–based geopolymer composites reinforced with biomass-derived *Phoenix sp*. fibers

M. G. Ranjith Kumar[1] · Ganeshprabhu Parvathikumar[2] · G. E. Arunkumar[3] · G. Rajeshkumar[4]

Received: 23 April 2024 / Revised: 23 June 2024 / Accepted: 10 July 2024

Abstract

Geopolymers are an inorganic cementitious material that is gaining attention for its exceptional mechanical qualities, strong thermal resistance, and low dielectric properties. However, the brittle failure and low ductility of geopolymers limit their use in load-bearing or structural applications. To overcome this challenge, the present work focused on improving the physico-mechanical, water, and thermal resistance properties of geopolymers by reinforcing untreated and alkali-treated (5, 10, and 15% concentrations) *Phoenix sp*. fibers. The outcomes revealed that the incorporation of *Phoenix sp*. fibers improved the performance of the geopolymer. In particular, the geopolymer reinforced with 10% alkali-treated fibers showed substantial improvement in their characteristics. The microstructural investigation demonstrated that the treated fibers formed a good interfacial bond with the geopolymers. In addition, load–deflection tests were conducted to examine the viability of the *Phoenix sp*. fiber–based geopolymer composites for structural applications. The findings of this study indicate that using alkali *Phoenix sp*. fibers as a fibrous material in the manufacturing of ecologically friendly and durable geopolymer concrete has a promising future in the construction sector.

Keywords Geopolymer · *Phoenix sp*. fiber · Alkali treatment · Mechanical properties · Interfacial bonding

1 Introduction

Ordinary Portland cement (OPC) has replaced wood as the preferred building material worldwide due to technological developments. OPC is in demand due to its tailored qualities, such as high comprehensiveness, durability, required mechanical strength for economic efficiency, water resistance, abundant ingredients across the globe, flexibility to mold into any desired form, and ease of acquisition. OPC output is rising 2.5% per year, from 2.3 billion tonnes in 2005 to 3.5 billion tonnes in 2020 and 3.7–4.4 billion tonnes by 2050. The manufacturing of OPC results in increased energy use and CO_2 emissions, which is a major concern [1, 2]. It is critical to identify a sustainable, high-performance alternative to OPC as a binder in order to reduce energy usage and greenhouse gas emissions. Alkali-activated geopolymers could be a better option for OPC [3]. These geopolymers make use of industrial by-products like fly ash and slag, which encourage recycling and reduce waste. Their ability to incorporate a variety of waste products contributes to their cost-effectiveness.

The ongoing growth of industrialization generates a significant amount of waste materials that are generated and dumped in landfills, including silica fume, furnace slag, fly ash, ash from rice husk, sugarcane bagasse, and palm oil [4–6]. Landfilling these waste items pollutes the environment. Fortunately, geopolymer requires high-alumino silicate raw ingredients. These resources reduce environmental pollution in the manufacture of geopolymers. Since these wastes are abundant and the demand for inexpensive housing will rise with population growth, using them would benefit the environment and economy. Geopolymers have been the subject of extensive global research and development, and they may soon become the best green construction material [7, 8].

✉ M. G. Ranjith Kumar
konguranjith17@gmail.com

[1] Department of Civil Engineering, Adithya Institute of Technology, Coimbatore, Tamil Nadu, India

[2] Department of Civil Engineering, Kamaraj College of Engineering and Technology, Virudhunagar, Tamil Nadu, India

[3] Department of Civil Engineering, Shree Venkateshwara Hi-Tech Engineering College, Erode, Tamil Nadu, India

[4] Department of Mechanical Engineering, PSG Institute of Technology and Applied Research, Coimbatore, Tamil Nadu, India

Published online: 19 July 2024

The impact of various types of fibers on the mechanical properties of geopolymer materials is extensive and multifaceted. Basalt, polypropylene, and natural fibers such as abaca hemp and coir can all enhance the strength, and toughness of geopolymers [9]. The incorporation of basalt and polypropylene fibers improved the bonding and ductility of the geopolymer concrete [10, 11]. On the other hand, adding hemp fibers (2 wt.%) increased the mechanical characteristics of the geopolymer composites. Similarly, adding 0.5 wt.% of cotton fiber improved the flexural qualities and fracture toughness of the geopolymer composites [12, 13].

Incorporating agro-waste material (natural fibers) into the geopolymer production process is one eco-solution that promotes the utilization of waste [14, 15]. Research has shown that by incorporating natural fibers into geopolymers, their bending strength, durability, and weight can be enhanced [16–18]. According to Onuaguluchi and Banthia [19] and Rojas et al. [20], the geopolymer composite (GPC) is well suited for applications in civil engineering, waste management, and building retrofitting owing to its exceptional properties. The *Phoenix sp*. plants can be found in many places, such as South Asia, Europe, Africa, and Malaysia. They grow along riverbanks, mangrove seashores, deserts, and semiarid soils. These plants are grown everywhere as decoration and then disposed of as waste. However, the petioles of this plant have a lot of fibers. These fibers are biodegradable, cheap, light, and easy to extract. From a sustainability perspective, the use of natural fibers encourages renewable resources. Furthermore, the more effective use of natural fibers in geopolymer composites contributes to waste reduction and enhances end-of-life recyclability. Therefore, utilizing the *Phoenix sp*. fibers for producing geopolymer-based composites promotes sustainable material development by improving natural fiber performance and encouraging the use of renewable resources without considerably increasing costs.

The fundamental challenge when making composites is the incompatibility of natural fibers and matrix materials. Natural fibers' hydrophilic features cause considerable moisture absorption, which can drastically affect their tensile behavior, as well as the durability of their composites [21]. Furthermore, pectin and waxy chemicals included in fibers hinder their interaction with the matrix. Surface changes to natural fibers are regarded as improving their bonding capabilities with the matrix material, resulting in superior overall composite qualities. Alkali treatment is one of the most commonly used procedures for treating natural fibers [22]. In our previous study, the raw *Phoenix sp*. fibers (PSFs) of different contents (1, 2, 3, and 4 wt.%) were reinforced into the geopolymer matrix or control matrix (CM), and their various properties were determined [23]. In order to increase the performance of the composites, alkali-treated PSFs were used in this work to make geopolymer composites. This geopolymer combination is a new and unexplored field of research. Therefore, this research focuses on the development of *Phoenix sp*. fiber–reinforced geopolymer composites (PRGC) and investigates the impact of chemical treatment on various properties of PRGC. Furthermore, the control matrix and untreated PRGC were produced and evaluated for comparison.

2 Materials and methods

2.1 Materials

The low-calcium fly ash (LCFA) collected from the thermal power plant is used in this research to make geopolymer concrete, and their chemical components are listed in Table 1. The aggregate material used was locally available, well-graded natural river sand. To minimize the impact of combined characteristics on the properties of geopolymers, only aggregates from a single source were used in this study. Figure 1 illustrates the size of the river sand fluctuation.

The PSFs extracted from their plant petioles through the water-retting process were used as reinforcement material. To enhance the interaction between PSFs and the matrix, the PSFs were treated with NaOH solutions at 5%, 10%, and 15% concentrations. During the process, the PSFs were immersed in the solution for 1 h, washed with running water, and dried in the normal environment for 48 h to eliminate moisture. SEM images of the PSFs showed that untreated fibers (Fig. 2a) had irregularities on their outer surface, while treated fibers (Fig. 2b) had a smoother surface and protrusions, increasing intrinsic bonding with bulk materials. Table 2 presents the characteristics of both untreated and treated PSFs.

Table 1 Chemical composition of LCFA

Chemical composition	Percentage
Silica	76.18
Alumina	15.42
Ferric oxide	3.19
Potassium oxide	1.95
Calcium oxide	0.91
Sulfuric anhydride	0.32
Magnesium oxide	0.25
Sodium oxide	0.15
Loss of ignition	1.63

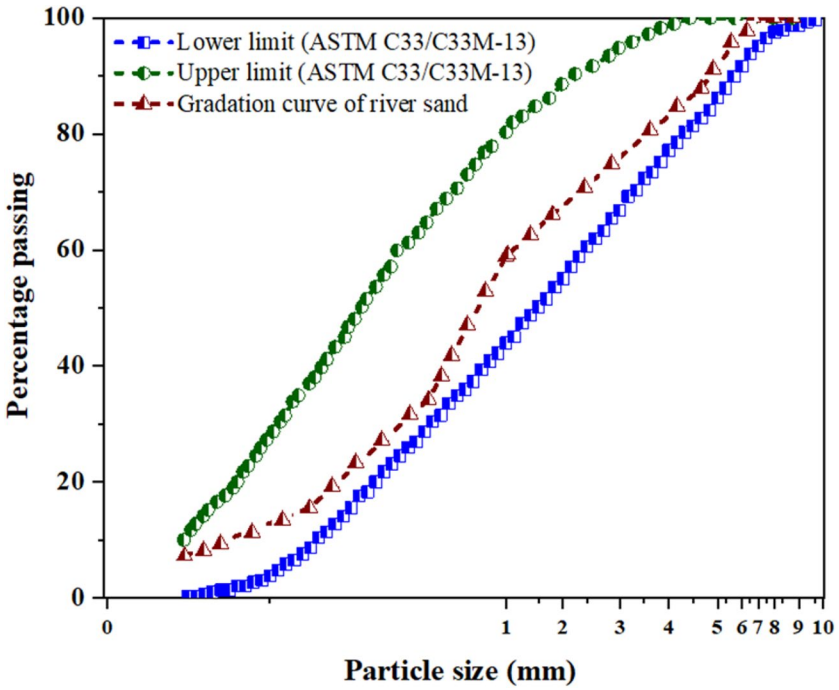

Fig. 1 Fluctuation in the size of the river sand

2.2 Methods

2.2.1 Preparation of samples

To examine the impact of fiber surface modification on different properties, geopolymer composites reinforced with untreated and treated PSFs were produced. An unreinforced geopolymer sample (control matrix) was also manufactured for comparison. To induce alkali activity in fly ash, a solution containing a combination of NaOH and Na_2SiO_3 was used. The content and modulus of the mixed alkali activator considered in this study are 10% and 1.5, respectively. To produce an effective geopolymer paste, fly ash, NaOH, and Na_2SiO_3 solutions were mixed for 6 min. The chopped PSFs with a length of 20 mm were then added to the mixture and stirred for 3 min to achieve homogeneity. After pouring the composites into the molds, they were vibrated for 10 s to improve compaction and then dried for 48 h at 65 °C. At last, the specimens were taken out from the mold and kept at 28 °C and 65% relative humidity till the time of testing. Table 3 provides the formulation of samples and their codes.

2.2.2 Experimental testings

A flow test was conducted in line with ASTM C1437-07 to evaluate the workability of the CM after PSF incorporation using Eq. 1.

$$Flow\ (F) = \frac{D - D_o}{D_o} \times 100 \tag{1}$$

where D denotes average base diameter and D_0 corresponds to original base bottom diameter.

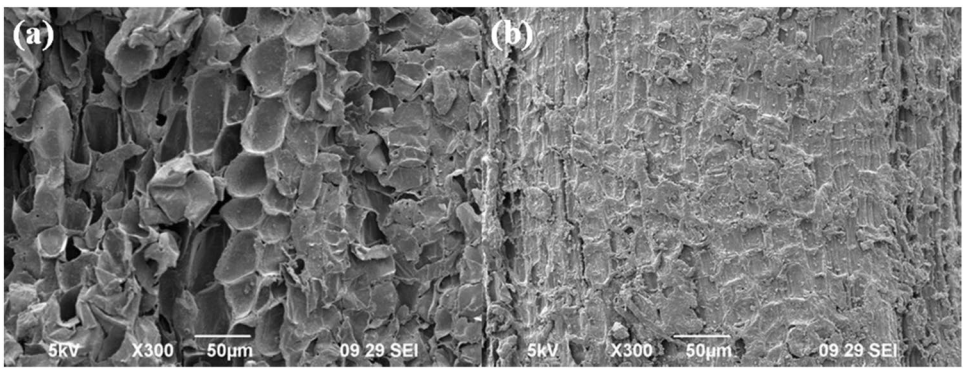

Fig. 2 SEM images of PSFs: **a** untreated and **b** NaOH-treated

Table 2 Characteristics of PSFs

Properties	Untreated	5% NaOH	10% NaOH	15% NaOH
Density (g/cm^3)	1.257	1.025	1.020	1.013
Cellulose (%)	76.13	63.31	66.57	62.94
Lignin (%)	4.29	29.98	30.10	32.88
Ash (%)	19.69	4.01	3.85	4.06
Moisture (%)	10.41	11.87	11.67	11.49
Tensile strength (MPa)	173.24	174.05	193.11	207.92

In accordance with the ASTM C-20 standard, the Archimedes method was employed to determine the bulk density and porosity of the manufactured samples. The mechanical strengths such as compression, splitting tensile, and flexural strengths of the specimens were determined as per ASTM C39/C39M, ASTM C496/C496M-17, and ASTM C78/C78M-16 standards, respectively, using an INSTRON-8801 Universal Testing Machine (UTM) with a 100-kN capacity.

The 100-mm cubic samples were prepared and subjected to a water absorption test as per the ASTM C642-13 standard. The test sample was immersed in water contained in a storage tank, and the test was conducted for 6, 12, 24, 48, and 72 h. The amount of water absorbed by the samples was computed using Eq. 2 [24].

$$Moisture\ absorption = \frac{m_f - m_i}{m_i} \tag{2}$$

where m_f and m_i denote mass of the sample prior to and after immersion in water, respectively.

In this work, the USPV of geopolymers and their composite samples (10-mm cube) were assessed as per ASTM C597-16 standard. To determine the thermal conductivity of 100-mm cube samples, a hot disk M1 analyzer manufactured by Thermal Instruments Ltd. was utilized [25].

To assess the fracture toughness of the material, $80 \times 20 \times 20$ mm^3 rectangular bars were tested. Using a 0.4-mm diamond blade, a crack with a l/W of 0.4 was made in each specimen, and the fracture toughness was computed using Eq. 3 [26].

Table 3 Formulation of samples and their codes

Sample code	Geopolymer (wt.%)	PSFs (wt.%)	Concentration of NaOH for fiber treatment (%)
CM	100	0	-
0TFC	98	2	0
5TFC	98	2	5
10TFC	98	2	10
15TFC	98	2	15

$$K_{IC} = \frac{PS}{Wt^{3/2}} \mathrm{f}\left(\frac{l}{t}\right) \tag{3}$$

where P is the peak load applied to the crack, S denotes span length, W is the specimen width, l is the crack length, t is the specimen thickness, and $f(l/t)$ for the polynomial geometrical correction factor given by Eq. 4 [27].

$$\mathrm{f}\left(\frac{l}{t}\right) = \frac{3\left(\frac{l}{t}\right)^{\frac{1}{2}}\left[1.99 - \left(\frac{l}{t}\right)\left(1 - \frac{l}{t}\right) \times \left(2.15 - 3.93\left(\frac{l}{t}\right) + 2.7\left(\frac{l}{t}\right)^2\right)\right]}{2\left(1 + \frac{2l}{t}\right)\left(1 - \frac{l}{t}\right)^{\frac{3}{2}}} \tag{4}$$

The load–deflection test was conducted to obtain the first crack, yield, and ultimate loads and their respective deflections, energy absorption capacity, toughness indices, ductility factor, and stiffness values of the prepared samples. The energy absorption capability of the samples ($100 \times 150 \times 1200$ mm^3) was quantified by adding the area under the load–deflection curves (LDC) up to the ultimate load. As per ASTM C1018, the toughness indices I_5 and I_{10} are computed using Eqs. 5 and 6, respectively [28].

$$I_5 = A_2/A_1 \tag{5}$$

$$I_{10} = A_3/A_1 \tag{6}$$

where A_1 is the area below the LDC up to the deflection of the first crack, and A_2 and A_3 correspond to the area below the LDC up to the deflection of 3 and 5.5 times the first crack, respectively.

The initial stiffness of the samples was obtained from the slope of the LDC. Equations (7) and (8) provide the pre-yield stiffness (K_1) and the post-yield stiffness (K_2) [29].

$$K_1 = P_y/\Delta_y \tag{7}$$

$$K_2 = \left(P_u - P_y\right)/\left(\Delta_u - \Delta_y\right) \tag{8}$$

where K_1 denotes the initial stiffness in kN.mm, K_2 corresponds to effective stiffness in kN.mm, P_y and P_u represent yield and ultimate load respectively in kN, and Δ_u and Δ_y indicate deflection at yield and ultimate point, respectively, in mm.

The surface of untreated and alkali-treated PSFs and fractured surfaces of geopolymer-based samples were investigated with ZEISS-SEM to understand fiber surface morphological changes and composite failure causes. For the analysis, a 15-kV accelerating voltage was applied.

3 Results and discussion

3.1 Flow property

The range of flow values for geopolymers and their composites is depicted in Fig. 3. It is observed that PRGC has less

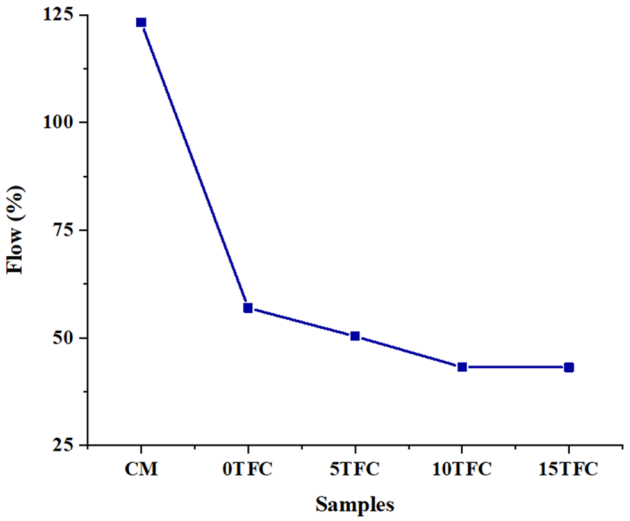

Fig. 3 Flowability of CM, untreated, and treated fiber–incorporated composites

flowability than CM. This could be attributed to composites' higher shear resistance to flow and increased composite stiffness with the inclusion of PSFs [30]. Further, the fibers have the potential to absorb a part of the mixing water, which decreases the total quantity of water available to maintain the flowability of the mixture. Moreover, the direct contact between the fibers and the CM enhances friction, hence diminishing the material's capacity to flow. Contrarily, when the composites were reinforced with 15% treated PSFs, there was an increase in their flowability. When fibers are treated with a highly concentrated alkali, the fiber surface is damaged, and the fiber becomes porous. This enhances the composite's flowability.

3.2 Bulk density and porosity

Figure 4 discloses that the density of the GPC is lower than that of the CM. This is because PSFs have a lower specific gravity. Furthermore, it is witnessed that the density of GPC reduces when treated PSFs are incorporated. The reason is that the increase in treatment concentration reduced the density of the fiber due to the removal of contaminants that existed on the surface of the fiber [31]. The amount of reduction in density with respect to an increase in concentration is displayed in Table 2. In this study, a 5% decrease in composite density is observed for each 5% increase in treatment concentration.

The porosity of composites is evidently greater than that of the control matrix (Fig. 4). This is due to the presence of voids and cracks on the fibers' surface. According to Alomayri et al. [27], the higher porosity of composites containing plant-based fibers is caused by the hydrophilicity of fibers, which generates voids in the fiber-matrix interface. Similarly, PSFs are also plant-based and highly hydrophilic, which is yet another reason for the increased porosity of the GPC as the fiber loadings increase. The increase in porosity will have an adverse effect on the composite's water absorption capability. Due to the capillary effect, micro-cracks formed at the interface by porosity promote water absorption. Consequently, the composites lose performance. Therefore, this issue should be addressed to increase the composite's durability. According to Su et al. [32] and Behforouz et al. [33], reinforcing pre-treatment fibers can reduce porosity in geopolymer composites, and the current work investigates the effect of treatment concentration on porosity. Further, the lower porosity of treated PSF–incorporated composites is attributed to the eradication of impurities that

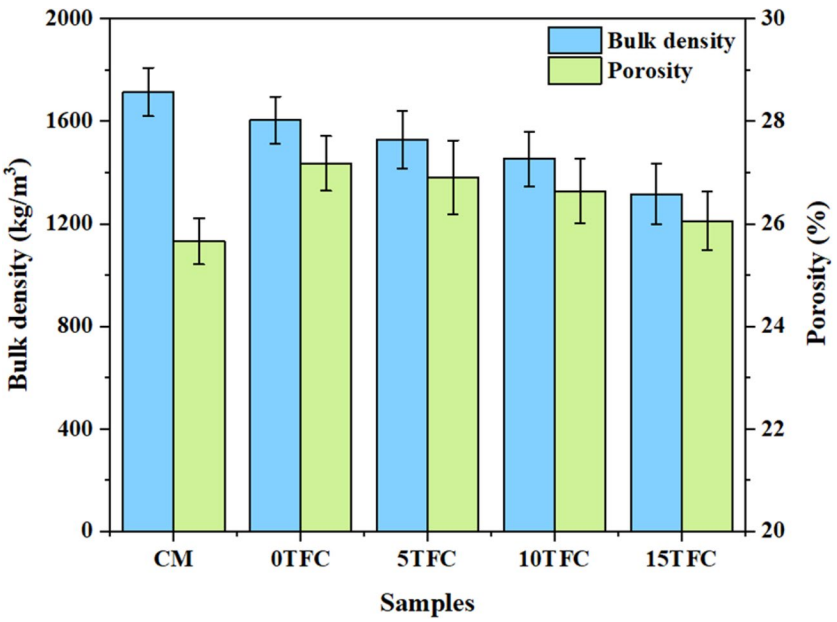

Fig. 4 Bulk density and porosity of CM and their composites

causes the fiber surface to become clean and rough, which facilitates better interfacial bonding between the composite constituents, resulting in a reduction in porosity. In addition, even though the reduction in porosity value is marginal, it will be advantageous in terms of water uptake behavior, mechanical qualities, and composite durability.

3.3 Mechanical properties

Figure 5 depicts the results of the investigation into the mechanical properties. The compressive strength of composites demonstrated greater values (31.26–34.83 MPa) than the CM (27.85 MPa), which is comparable with the findings of prior research [30, 34]. It is worth noting that the compressive strength of GPC increased when the treated fibers were loaded. This is because the NaOH treatment can get rid of unwanted materials and make the reinforcement's surface rougher, which makes it easier for the composite parts to stick together[35]. Specifically, composites containing 10% treated fiber displayed the greatest compressive strength of 34.83 MPa, which was 25.06% greater than the standard sample. The composites containing 15% treated fiber have a somewhat lower compressive strength than the composites containing 10% treated fiber, but it is still greater than the composites containing untreated fiber and the CM. The improvement in compressive strength of GPC was also conveyed in the literature [36, 37].

The test results for splitting tensile strength (STS) showed that the inclusion of PSFs significantly increased the STS of the geopolymer. The improvement is the result of the fiber's excellent tensile characteristics. Moreover, the existence of reinforcement in CM simplified stress transfer through the interface, thereby increasing the load-carrying capability of GPC and allowing for the achievement of greater strength [34]. Further, the existence of reinforcement in CM simplified stress transfer through the interface, thereby increasing GPC's load-carrying capability and allowing for greater strength. This is due to the existence of protrusions on the treated fiber surface, as shown in SEM images of treated fibers (Fig. 5). These protrusions serve as a mechanical interlocking mechanism during tensile loading, hence increasing the load-carrying capability of composites[38]. In the current investigation, composites containing 10% treated fiber had a tensile strength of 99.21% more than the control matrix. The decline in tensile strength of 15% treated PSF–added composites is attributable to the weakening of fibers after treatment at increasing alkali concentrations.

The flexural strength of GPC is noted to be greater than the CM. This is because the existence of PSFs can efficiently support increased load, delaying the formation of microcracks and enhancing flexural strength. On the other hand, the alkali treatment enhances the PRGC's flexural strength. In particular, the geopolymer containing 10% treated fiber exhibited greater flexural strength than the control matrix and untreated fiber composites by 123.35% and 53.52%, respectively. This is because the treatment stimulates the precipitation of soluble sugars in advance, reduces the polymerization reaction's influence, and creates coarser fiber surfaces, resulting in strong fiber-matrix adhesion. Zhou et al. [35] determined that alkali treatment increased the flexural strength of GPC-containing cotton stalk fiber by 11.5%. Also, Yan et al. [39] identified that the NaOH treatment augmented the flexural strength of coir fiber–loaded composites by 21.4%. The current study's findings are consistent with the aforementioned literature.

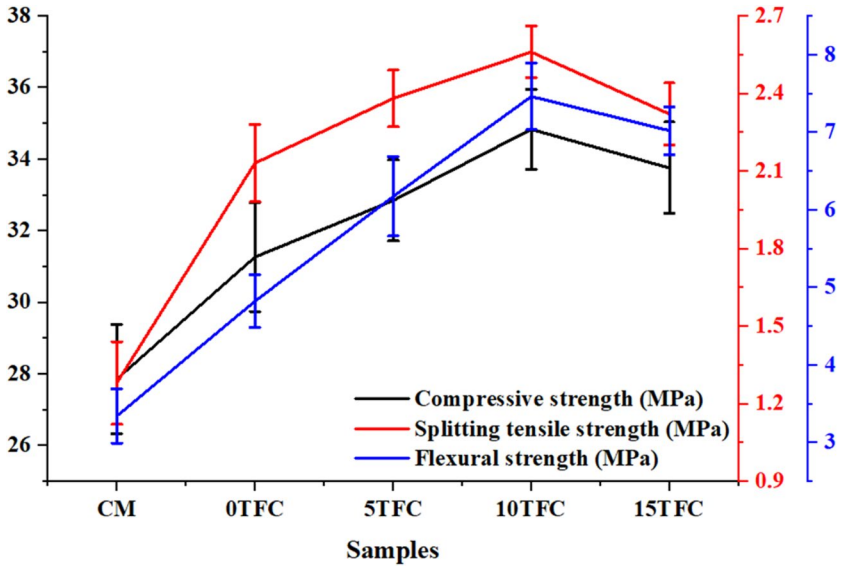

Fig. 5 Mechanical properties of CM, untreated, and treated fiber–incorporated composites

3.4 Water absorption

The proportion of water absorbed by the CM and their composites is presented in Fig. 6. It is apparent that all composites absorb more water than CM. This may be a result of the hydrophilicity of PSF [40] and the increased interfacial area among PSF and CM. Utilizing surface-treated or surface-coated fibers reduces the water absorption rate. In this context, surface-modified PSFs were reinforced, and their water absorption behavior in relation to treatment concentration was investigated. The outcomes reveal that the water uptake by the GPC decreases with increasing treatment concentrations up to 10% and tends to increase with increasing treatment concentrations up to 15%. It is possible that the pre-treatment of the reinforcements aided their bonding with the base material, thereby reducing the pores and voids. The water absorption of composites containing 5%, 10%, and 15% treated fibers is reduced by 13.55%, 20.33%, and 16.95% respectively, compared to composites containing untreated fibers. Therefore, it was ascertained that the pre-treatment of PSF considerably reduces the water absorption rate of GPC. Similar patterns of outcomes were reported for pre-treated cotton stalk–reinforced geopolymer composites [35] and pre-treated rice straw–incorporated geopolymer composites [24].

3.5 Ultrasonic pulse velocity

Figure 7a illustrates the USPV results of CM and their composites. It is evident that the inclusion of PSFs increased the USPV. This is because ultrasonic waves travel through fibers faster than through geopolymers. Furthermore, it is clear that the composite's USPV increased as the concentration of alkali treatment increased. It is anticipated that, after treatment, the fibers will stiffen and form strong interfacial bonds with the matrix, thereby increasing the speed of the ultrasonic waves. A slight decrease in USPV is observed in composites containing fibers treated with a 15% concentration. It is ascribed to fiber damage occurring due to higher concentrations of alkaline solution, resulting in an increase in the porosity of composites. Finally, the optimal concentration of treatment is determined to be 10%, which offers 8.1%, 5.16%, and 2.5% more USPV than the concentrations of 0%, 5%, and 15%, respectively. Furthermore, it is worth noting that the USPV improvement is only marginal. A significant improvement in USPV could be obtained by using nanoparticles as secondary reinforcements.

In addition, a strong correlation exists between USPV and the compressive strength of materials. Figure 7b depicts a correlation established between USPV and the compressive strength of the samples tested. The current investigation revealed a linear relationship between these parameters with a correlation coefficient (R^2) of 0.98, which is consistent with previous studies [41, 42].

3.6 Thermal conductivity (TC)

The thermal conductivities of geopolymers and their composites (Fig. 8a) range from 0.28 to 0.48 W/m K. The outcomes revealed that the inclusion of PSF decreased the TC of GPC, which is in agreement with the density results previously described [43, 44]. The decrease in the TC of CM with

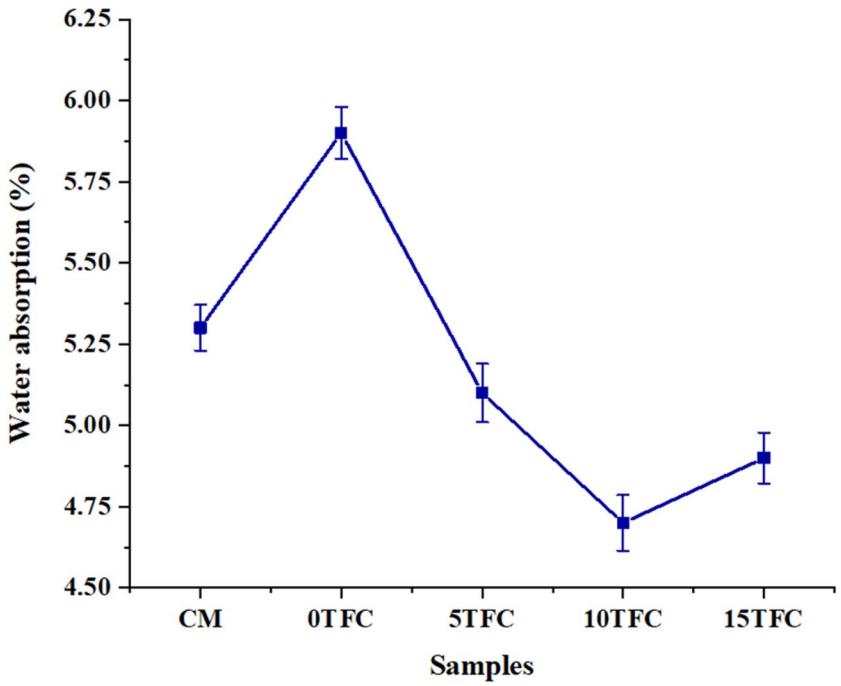

Fig. 6 Water absorption of CM, untreated, and treated fiber–incorporated composites

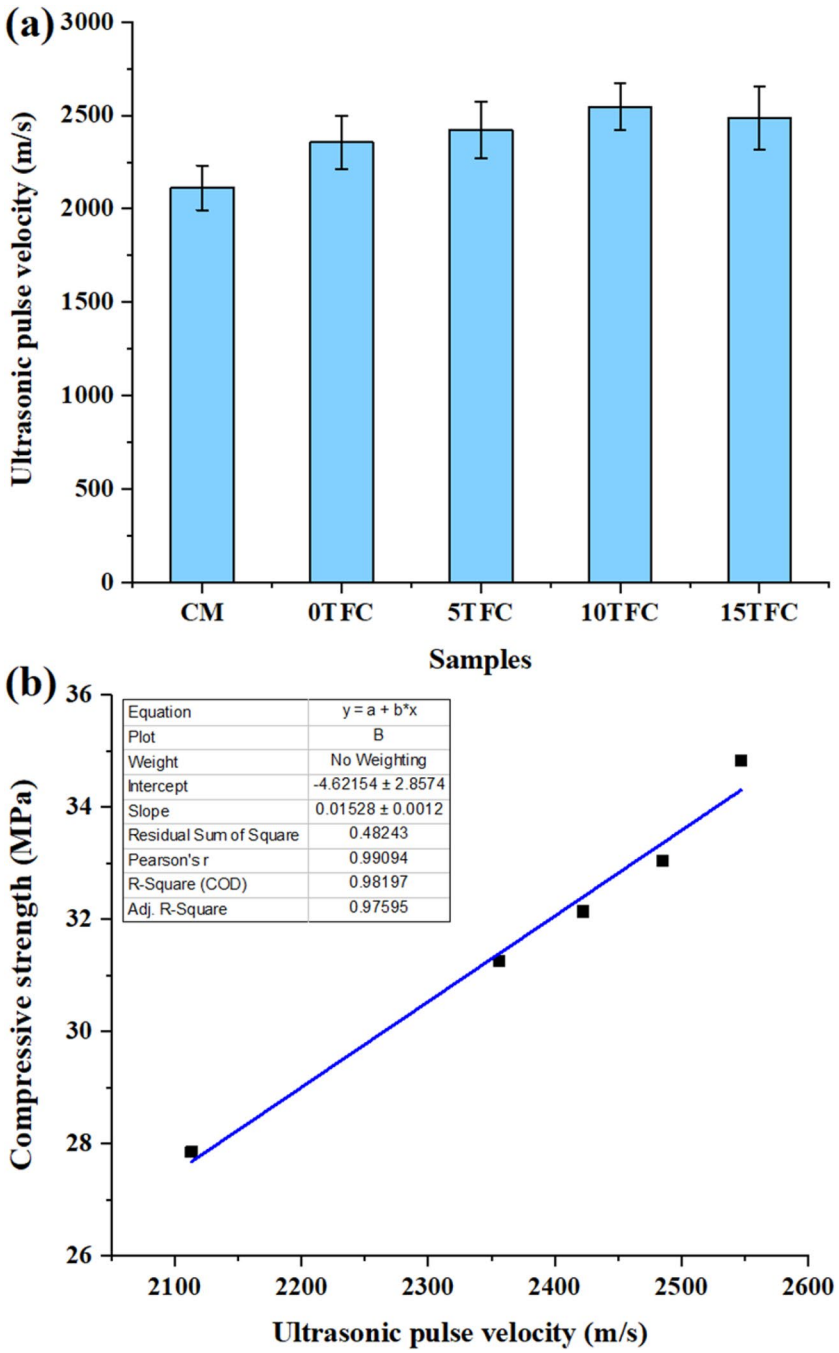

Fig. 7 UPSV: **a** CM, untreated, and treated fiber–incorporated composites, and **b** correlation between USPV and the compressive strength

the addition of PSFs can be ascribed to several factors: (i) PSFs exhibit a lower TC when compared to the CM. When these fibers are added to the geopolymer, they function as insulating materials, which leads to a decrease in the overall TC of the composite, (ii) the interaction between the PSFs and CM can create interfaces that disrupt the flow of heat. These interfaces have the ability to disperse and reflect thermal energy, resulting in a decrease in the TC, and (iii) the heterogeneous nature of the PSF-reinforced GPC results in less effective heat transfer compared to a homogeneous material, resulting in a reduction in TC. Furthermore, as the alkali treatment concentration increased, the TC decreased. This occurs due to the decreased bulk density of the treated fiber GPC, as described in Sect. 3.2. The composites containing 15% treated fiber had 41.66% less thermal conductivity than the companion control matrix. Finally, this variation in values had a positive effect on the TC of GPC, suggesting that thermal insulation can be enhanced by using GPC with low TC [45, 46]. In addition, the bulk density of both the CM and the composites is closely related to their thermal conductivity. Figure 8b depicts the relationship between TC and the bulk density of the tested materials. Consistent with

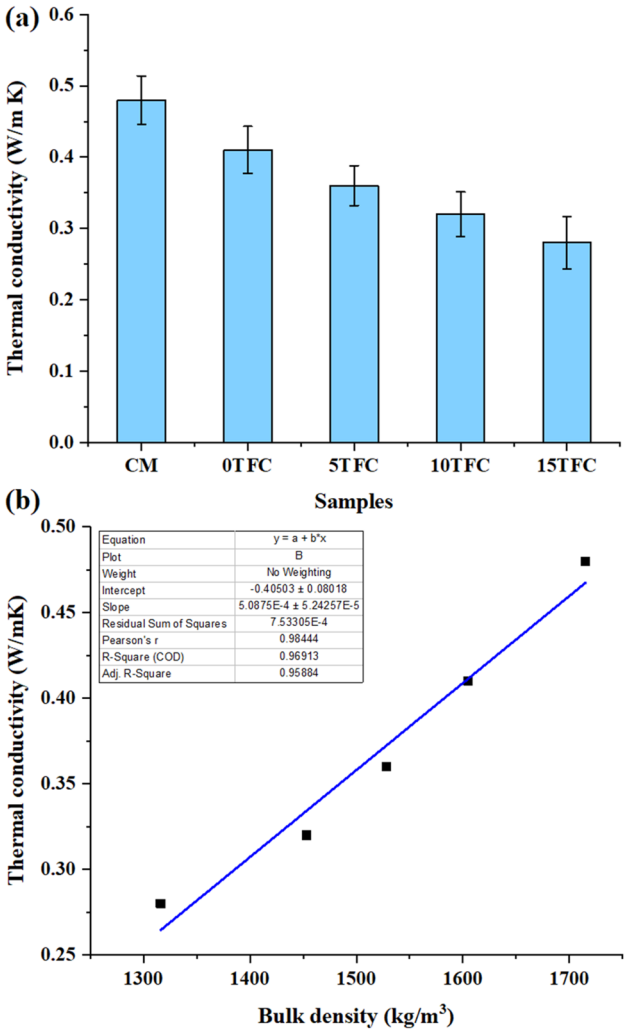

Fig. 8 Thermal conductivity of **a** CM, untreated, and treated fiber–incorporated composites, and **b** relationship between TC and the bulk density

prior research, the present study found a linear correlation between these variables, with an R^2 value of 0.96 [34, 43].

3.7 Fracture toughness (FRTS)

Figure 9 depicts the effect of chemical treatment on FRTS of PRGC. The inclusion of PSF increased the FRTS of the CM from 0.57 to 0.9 MPa $m^{1/2}$. This could be due to the energy-absorbing qualities of the PSF [27, 47]. Moreover, the existence of PSFs can modify the path of cracks, leading to their deviation, division, or blunting. Consequently, this raises the amount of energy required for crack propagation, thereby improving the FRTS of the composites. The results also indicated that the FRTS increased with an increase in the treatment concentration up to 10% and decreased with a further increase in the treatment concentration. The enhanced FRTS of geopolymers can be related to the strong bonding between the treated fibers (5% and 10%) and geopolymer. Under the application of stress, the primary mode of failure in composite materials is fiber fracture, which requires a significant amount of time and energy. As a result, there is an increase in fracture toughness, which enhances the material's strength and durability. The composites added with 10% treated fiber exhibit 25%, 13.92%, and 2.27% higher fracture toughness when compared to untreated, 5%, and 15% treated PFRG, respectively. Because of the higher concentration of alkali, the 15% treated PSF has damage and cracks on its surface, which contributes to the reduction in the fracture toughness of the GPC.

3.8 Load–deflection analysis

3.8.1 Load–deflection curve

Figure 10 illustrates the impact of untreated and alkali-treated PSF additions on the load–deflection behavior of CM and their composites. The results showed that using PSFs considerably enhanced post-cracking behavior, which contributes to increasing the area under the non-linear section of the LDC and hence the amount of energy absorbed by the material during fracture. The reinforcements can change the behavior of reinforced geopolymers from linear to ductile [28, 48]. The present work results clearly indicated that the composites have a 2–2.5 times higher ultimate load when compared to the control matrix (12.09 kN).

3.8.2 Energy absorption capacity

Figure 11 exemplifies that the control matrix has negligible energy absorption capability when compared to fiber-reinforced geopolymers (Fig. 11a and b). This may be attributed to the enhanced load-bearing capacity of GPC with the inclusion of fibers. Furthermore, the beam deflects more when fibers are added to the geopolymer, which improves the composite's ductility. Due to their better interfacial bonding, treated fiber–added composites (Fig. 11c, d) exhibited a greater energy-absorbing capacity than untreated fiber–added composites.

3.8.3 Toughness indices

The I_5 and I_{10} toughness indices of CM and their PSF-based composites are given in Table 4. It is observed that the composite's toughness exceeds that of the control matrix. This could be related to the reinforcing effect of PSFs. Furthermore, improved bonding between composite

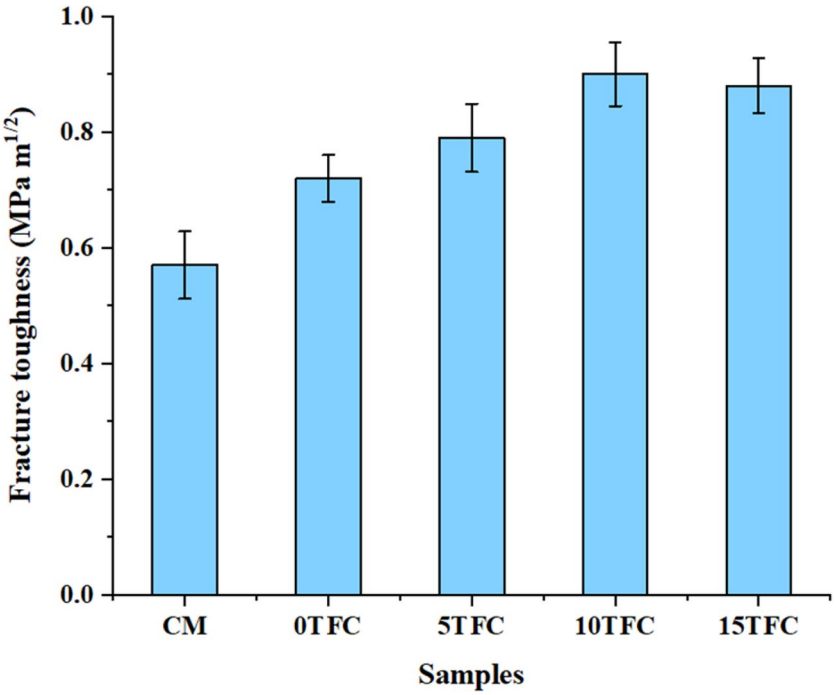

Fig. 9 Fracture toughness of CM and their composites

sections contributes to the increased load-bearing capability of treated fiber–included composites. This is the fundamental reason for the composites' increased durability. However, in the present work, a marginal improvement in toughness indices is evidenced between the untreated and alkali-treated PSF–incorporated composites.

3.8.4 Stiffness

Table 5 displays the initial and effective stiffness of the samples. The control matrix has a higher initial stiffness than the GPC with untreated fiber additions. This could be related to the brittle behavior of the control matrix, which results in

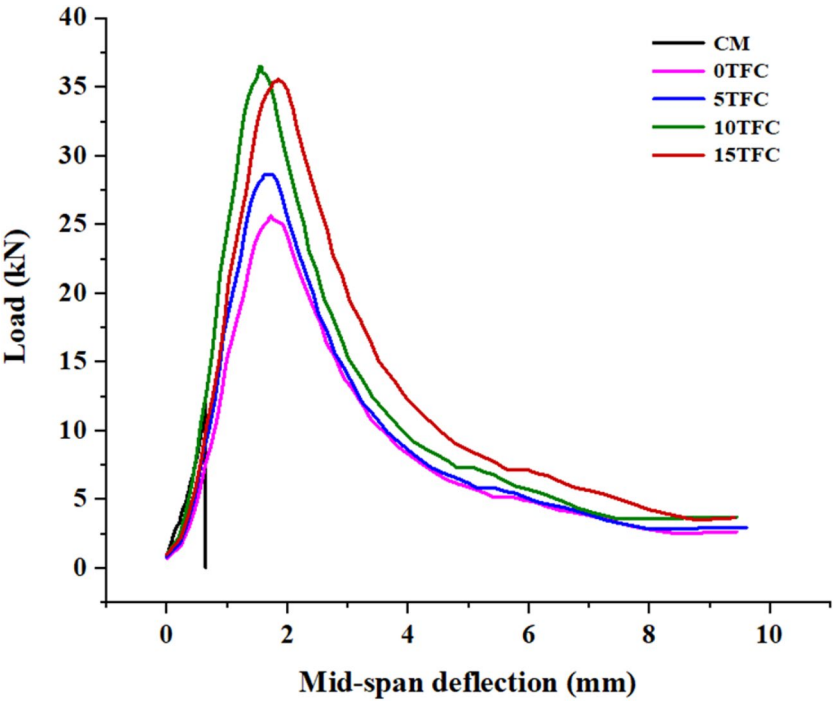

Fig. 10 LDC of CM, untreated, and treated fiber–incorporated composites

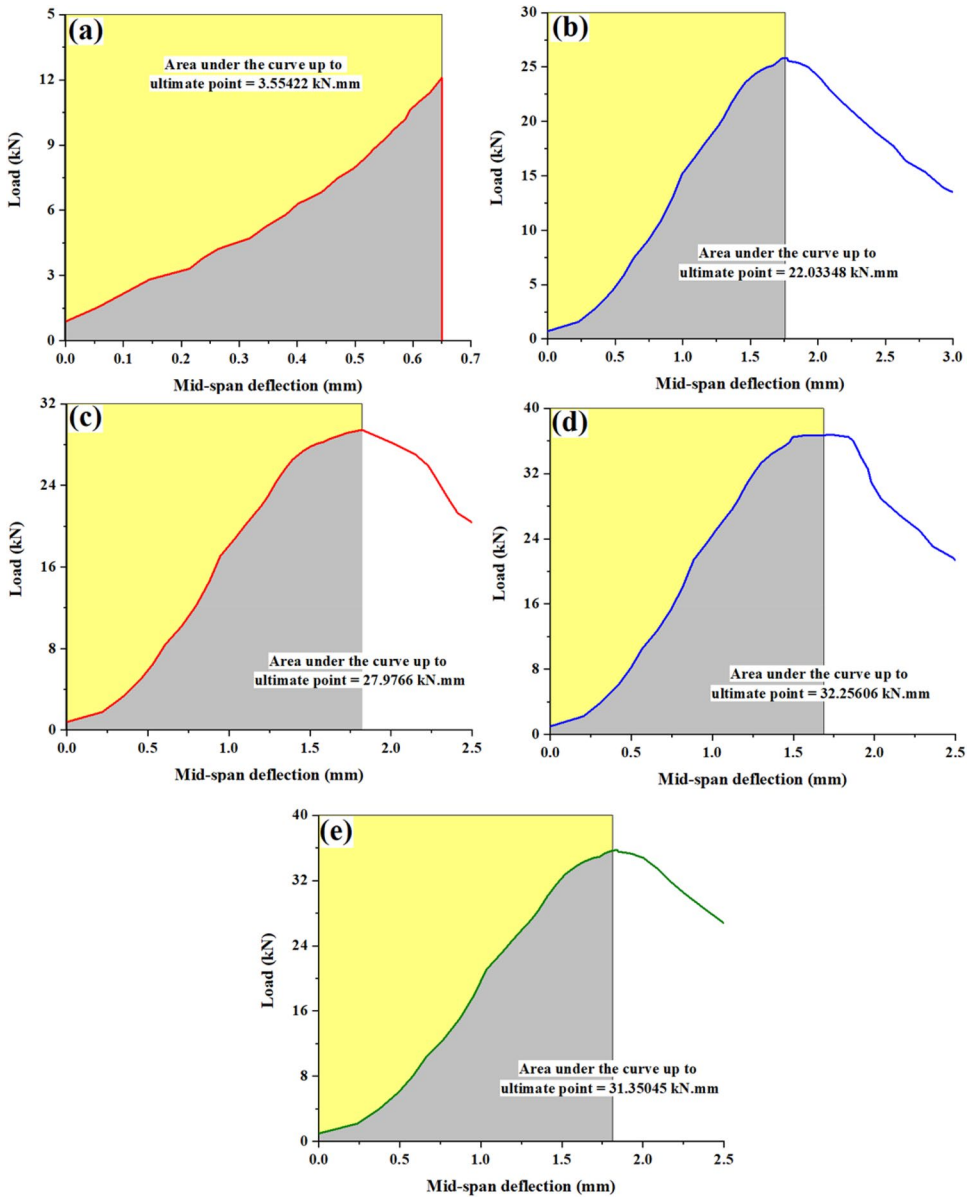

Fig. 11 Energy absorbing capacity of **a** CM, **b** 0TFC, **c** 5TFC, **d** 10TFC, and **e** 15TFC

reduced deflection. The inclusion of low-density PSFs turns the brittle behavior of the CM into a ductile behavior, resulting in a greater amount of deflection. This effect drastically reduced the composite's initial rigidity. In the preceding sections, it was stated that the pre-treatment of fibers improved their stiffness, which is reflected in the results of composites including treated fibers. In the present study, the initial stiffness values of treated PRGC are marginally higher than those of untreated PRGC.

Table 4 I_5 and I_{10} toughness indices of CM and their composites

Toughness indices	CM	0TFC	5TFC	10TFC	15TFC
I_5	6.29	14.54	14.86	14.89	13.83
I_{10}	13.93	32.17	32.43	33.74	29.58

3.9 Morphological analysis

The interaction between elements of GPC was examined using SEM micrographs. In order to enhance the efficiency of energy absorption in GPC, it is vital to have an appropriate interface between the composite elements [49]. The SEM image (Fig. 12a) displayed uneven stripes and a rougher surface, which facilitated the attachment of the PSFs to the GPM [34]. The void formations resulting from fiber pull-outs, inadequate bonding between parts, and fractures observed in Fig. 12b demonstrated the poor interfacial bonding between the PSFs and GPM. During

Table 5 Initial and effective stiffness of different samples

Reinforcement	Quantity	P_y (kN)	P_u (kN)	Δ_y (mm)	Δ_u (mm)	K_1(kN.mm)	K_2(kN.mm)
None	-	7.48	12.09	0.26	0.65	28.76	11.82
Untreated fiber	2 wt. %	14.93	25.87	0.99	1.76	15.08	14.20
Alkali-treated fiber	5% NaOH	16.30	29.47	0.93	1.82	17.53	14.79
	10% NaOH	21.05	36.74	0.86	1.68	24.47	19.13
	15% NaOH	20.06	35.77	1.01	1.81	19.86	19.63

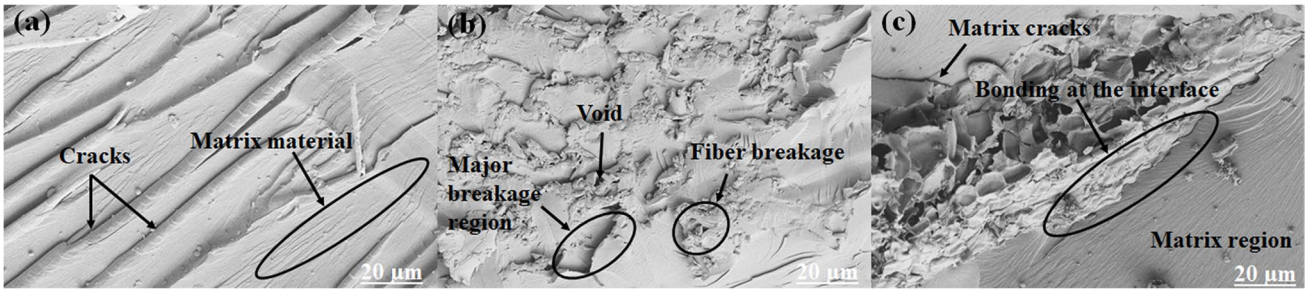

Fig. 12 SEM images of samples: **a** CM, **b** 0TFC, and **c** 10TFC

fiber pull-outs, microcracks will develop in close proximity to the void regions. These fractures will then propagate under load, ultimately resulting in the failure of composites. This could be overcome by improving the interfacial bonding between the composite elements by incorporating the treated fibers. The current study demonstrates that the alkali-treated fibers establish a strong bond with the GPM (Fig. 12c), which contributes to the enhanced overall performance of composites.

4 Conclusions

In this study, the effect of alkali treatments on the physico-mechanical, water, and thermal resistance properties of geopolymers and their composites was investigated. The experimental data revealed that the addition of PSFs to GPM reduces their flowability due to the increased shear resistance to flow in composites. The porous characteristics of the reinforcement materials cause the bulk density of composites to decline. The porosity of treated PSF–added composites showed a decreasing trend owing to the close packing of composite elements. The incorporation of alkali-treated PSFs increased the mechanical properties, ultrasonic pulse velocity, and fracture toughness of the composites due to improved interface bonding and effective stress transfer that occurred at the interface. On the other hand, the incorporation of treated fibers reduced the water absorption rate and thermal conductivity of the composites. Incorporating PSFs into GPM increased the ultimate load and permitted substantial deformation without breaking during bending tests, demonstrating the ductile fracture behavior of composites. Finally, this research showed that 10% treated PSFs in geopolymer composites could potentially serve as an alternative material for thermal insulation and construction applications.

Although composites containing alkali-treated PSFs exhibit enhanced interfacial bonding, their performance can be further enhanced by incorporating nano-clay as a secondary reinforcement material. Using nano-clay, even in minimal quantities, can result in improved material efficiency and possible future cost reductions. Therefore, geopolymer composites incorporating 10% alkali-treated PSFs and nano-clay could be cast and subjected to detailed characterization studies.

Author contribution Conceptualization and methodology: M.G. Ranjith kumar and Ganeshprabhu Parvathikumar.

Experiments and interpretation of data: M.G. Ranjith kumar and G. Rajeshkumar.

Writing—original draft: G.E. Arunkumar.

Review and editing: M.G. Ranjith kumar.

Proofreading of final version: G. Rajeshkumar.

Declarations

Ethical approval This declaration is not applicable.

Competing interests The authors declare no competing interests.

References

1. Yang H, Liu L, Yang W et al (2022) A comprehensive overview of geopolymer composites: a bibliometric analysis and literature review. Case Stud Constr Mater 16. https://doi.org/10.1016/j.cscm.2021.e00830
2. Benhelal E, Zahedi G, Shamsaei E, Bahadori A (2013) Global strategies and potentials to curb CO2 emissions in cement industry. J Clean Prod 51:142–161. https://doi.org/10.1016/j.jclepro.2012.10.049
3. Liu J, Xincheng Su FY (2022) Experimental investigation on the effect of geopolymer adhesive on the bond behavior between CFRP and concretes. Polym Compos 43:3259–3275
4. Cui Y, Hao H, Li J et al (2022) Structural behavior and vibration characteristics of geopolymer composite lightweight sandwich panels for prefabricated buildings. J Build Eng 57. https://doi.org/10.1016/j.jobe.2022.104872
5. Lv C, Liu J, Guo G et al (2022) The mechanical properties of plant fiber-reinforced geopolymers: a review. Polymers 14:1–23. https://doi.org/10.3390/polym14194134
6. Narattha C, Wattanasiriwech S, Wattanasiriwech D (2022) Thermal and mechanical characterization of fly ash geopolymer with aluminium chloride and potassium hydroxide treated hemp shiv lightweight aggregate. Constr Build Mater 331. https://doi.org/10.1016/j.conbuildmat.2022.127206
7. Jiang Z, Zhao C, Xie J, Tan Y, Shixin Li ZL (2023) Shear performance degradation of basalt fiber-reinforced polymer bars in seawater environments: coupled effects of seawater sea-sand geopolymer mortar coatings and sustained loading. Polym Compos 44:8465–8483
8. Zaid O, Martínez-García R, Abadel AA et al (2022) To determine the performance of metakaolin-based fiber-reinforced geopolymer concrete with recycled aggregates. Arch Civ Mech Eng 22:1–14. https://doi.org/10.1007/s43452-022-00436-2
9. Mashayekhi A, Hassanli R, Zhuge Y et al (2024) Synergistic effects of fiber hybridization on the mechanical performance of seawater sea-sand concrete. Constr Build Mater 416:135087. https://doi.org/10.1016/j.conbuildmat.2024.135087
10. Yang Z, Lu F, Zhan X et al (2024) Mechanical properties and mesoscopic damage characteristics of basalt fibre-reinforced seawater sea-sand slag-based geopolymer concrete. J Build Eng 84:108688. https://doi.org/10.1016/j.jobe.2024.108688
11. Yang Z, Zhan X, Zhu H et al (2024) Eco-sustainable design of seawater sea-sand slag-based geopolymer mortars incorporating ternary solid waste. Constr Build Mater 431:136512. https://doi.org/10.1016/j.conbuildmat.2024.136512
12. Alomayri T, Shaikh FUA, Low IM (2013) Characterisation of cotton fibre-reinforced geopolymer composites. Compos Part B Eng 50:1–6. https://doi.org/10.1016/j.compositesb.2013.01.013
13. Maichin P, Suwan T, Jitsangiam P et al (2020) Effect of self-treatment process on properties of natural fiber-reinforced geopolymer composites. Mater Manuf Process 35:1120–1128. https://doi.org/10.1080/10426914.2020.1767294
14. Akhter F, Soomro SA, Jamali AR, Chandio ZA, MS& MA, (2023) Rice husk ash as green and sustainable biomass waste for construction and renewable energy applications: a review. Biomass Convers Biorefinery 13:4639–4649
15. Mohanad Yaseen Abdulwahid, Abayomi Adewale Akinwande, Maksim Kamarou et al (2023) The production of environmentally friendly building materials out of recycling walnut shell waste: a brief review. Biomass Convers Biorefinery 1–10. https://doi.org/10.1007/s13399-023-04760-2
16. Correia EA, Torres SM, Alexandre MEO et al (2013) Mechanical performance of natural fibers reinforced geopolymer composites. Mater Sci Forum 758:139–145. https://doi.org/10.4028/www.scientific.net/MSF.758.139
17. Silva G, Kim S, Bertolotti B et al (2020) Optimization of a reinforced geopolymer composite using natural fibers and construction wastes. Constr Build Mater 258:1–12. https://doi.org/10.1016/j.conbuildmat.2020.119697
18. Camargo MM, Taye EA, Roether JA et al (2020) A review on natural fiber-reinforced geopolymer and cement-based composites. Materials (Basel) 13:1–29. https://doi.org/10.3390/ma13204603
19. Onuaguluchi O, Banthia N (2016) Plant-based natural fibre reinforced cement composites: a review. Cem Concr Compos 68:96–108. https://doi.org/10.1016/j.cemconcomp.2016.02.014
20. Rojas M, Silva G, Javier Nakamatsu RA, Suyeon K (2022) Alkali-treated Agave americana fiber for reinforcement of fly ash-based geopolymers. J Nat Fibers 19:12647–12663
21. Preethikaharshini J, Naresh K, Rajeshkumar G et al (2022) Review of advanced techniques for manufacturing biocomposites: non-destructive evaluation and artificial intelligence-assisted modeling. J Mater Sci 57:16091–16146. https://doi.org/10.1007/s10853-022-07558-1
22. Karthi N, Kumaresan K, Rajeshkumar G et al (2021) Tribological and thermo-mechanical performance of chemically modified Musa acuminata/Corchorus capsularis reinforced hybrid composites. J Nat Fibers 00:1–14. https://doi.org/10.1080/15440478.2020.1870614
23. Ranjithkumar MG, Chandrasekaran P, Rajeshkumar G (2022) Characterization of sustainable natural fiber reinforced geopolymer composites. Polym Compos 43:3691–3698. https://doi.org/10.1002/pc.26646
24. Huang Y, Tan J, Xuan X et al (2021) Study on untreated and alkali treated rice straw reinforced geopolymer composites. Mater Chem Phys 262:1–9. https://doi.org/10.1016/j.matchemphys.2021.124304
25. Colangelo F, Roviello G, Ricciotti L et al (2018) Mechanical and thermal properties of lightweight geopolymer composites. Cem Concr Compos 86:266–272. https://doi.org/10.1016/j.cemconcomp.2017.11.016
26. Low IM, McGrath M, Lawrence D et al (2007) Mechanical and fracture properties of cellulose-fibre-reinforced epoxy laminates. Compos Part A Appl Sci Manuf 38:963–974. https://doi.org/10.1016/j.compositesa.2006.06.019
27. Alomayri T, Assaedi H, Shaikh FUA, Low IM (2014) Effect of water absorption on the mechanical properties of cotton fabric-reinforced geopolymer composites. J Asian Ceram Soc 2:223–230. https://doi.org/10.1016/j.jascer.2014.05.005
28. Natali A, Manzi S, Bignozzi MC (2011) Novel fiber-reinforced composite materials based on sustainable geopolymer matrix. Procedia Eng 21:1124–1131. https://doi.org/10.1016/j.proeng.2011.11.2120
29. Mamdouh H, Ali AM, Osman MA et al (2022) Effects of size and flexural reinforcement ratio on ambient-cured geopolymer slag concrete beams under four-point bending. Buildings 12. https://doi.org/10.3390/buildings12101554
30. Ranjbar N, Talebian S, Mehrali M et al (2016) Mechanisms of interfacial bond in steel and polypropylene fiber reinforced

geopolymer composites. Compos Sci Technol 122:73–81. https://doi.org/10.1016/j.compscitech.2015.11.009
31. Rajeshkumar G, Hariharan V, Scalici T (2016) Effect of NaOH treatment on properties of Phoenix sp. fiber. J Nat Fibers 13:702–713. https://doi.org/10.1080/15440478.2015.1130005
32. Su Z, Guo L, Zhang Z, Duan P (2019) Influence of different fibers on properties of thermal insulation composites based on geopolymer blended with glazed hollow bead. Constr Build Mater 203:525–540. https://doi.org/10.1016/j.conbuildmat.2019.01.121
33. Behforouz B, Balkanlou VS, Naseri F et al (2020) Investigation of eco-friendly fiber-reinforced geopolymer composites incorporating recycled coarse aggregates. Int J Environ Sci Technol 17:3251–3260. https://doi.org/10.1007/s13762-020-02643-x
34. Wongsa A, Kunthawatwong R, Naenudon S et al (2020) Natural fiber reinforced high calcium fly ash geopolymer mortar. Constr Build Mater 241. https://doi.org/10.1016/j.conbuildmat.2020.118143
35. Zhou B, Wang L, Ma G et al (2020) Preparation and properties of bio-geopolymer composites with waste cotton stalk materials. J Clean Prod 245. https://doi.org/10.1016/j.jclepro.2019.118842
36. Hu Y, Liang S, Yang J et al (2019) Role of Fe species in geopolymer synthesized from alkali-thermal pretreated Fe-rich Bayer red mud. Constr Build Mater 200:398–407. https://doi.org/10.1016/j.conbuildmat.2018.12.122
37. Qaidi S, Najm HM, Abed SM et al (2022) Fly ash-based geopolymer composites: a review of the compressive strength and microstructure analysis. Materials (Basel) 15. https://doi.org/10.3390/ma15207098
38. Rajeshkumar G, Hariharan V, Indran S et al (2021) Influence of sodium hydroxide (NaOH) treatment on mechanical properties and morphological behaviour of Phoenix sp. fiber/epoxy composites. J Polym Environ 29:765–774. https://doi.org/10.1007/s10924-020-01921-6
39. Yan L, Chouw N, Huang L, Kasal B (2016) Effect of alkali treatment on microstructure and mechanical properties of coir fibres, coir fibre reinforced-polymer composites and reinforced-cementitious composites. Constr Build Mater 112:168–182. https://doi.org/10.1016/j.conbuildmat.2016.02.182
40. Rajeshkumar G (2020) An experimental study on the interdependence of mercerization, moisture absorption and mechanical properties of sustainable Phoenix sp. fibre-reinforced epoxy composites. J Ind Text 49:1233–1251. https://doi.org/10.1177/1528083718811085
41. Shankar S, Joshi HR (2014) Comparison of concrete properties determined by destructive and non-destructive tests. J Inst Eng 10:130–139. https://doi.org/10.3126/jie.v10i1.10889
42. Ghosh R, Sagar SP, Kumar A et al (2018) Estimation of geopolymer concrete strength from ultrasonic pulse velocity (UPV) using high power pulser. J Build Eng 16:39–44. https://doi.org/10.1016/j.jobe.2017.12.009
43. Khedari J, Suttisonk B, Pratinthong N, Hirunlabh J (2001) New lightweight composite construction materials with low thermal conductivity. Cem Concr Compos 23:65–70. https://doi.org/10.1016/S0958-9465(00)00072-X
44. Mounika M, Ramaniah K, Ratna Prasad AV et al (2012) Thermal conductivity characterization of bamboo fiber reinforced polyester composite. J Mater Environ Sci 3:1109–1116
45. Khedari J, Nankongnab N, Hirunlabh J, Teekasap S (2004) New low-cost insulation particleboards from mixture of durian peel and coconut coir. Build Environ 39:59–65. https://doi.org/10.1016/j.buildenv.2003.08.001
46. Lisowski P, Glinicki MA (2023) Promising biomass waste–derived insulation materials for application in construction and buildings. Biomass Convers Biorefinery. https://doi.org/10.1007/s13399-023-05192-8
47. Farhan KZ, Johari MAM, Demirboğa R (2021) Impact of fiber reinforcements on properties of geopolymer composites: a review. J Build Eng 44. https://doi.org/10.1016/j.jobe.2021.102628
48. Toutanji H, Xu B, Gilbert J, Lavin T (2010) Properties of poly(vinyl alcohol) fiber reinforced high-performance organic aggregate cementitious material: converting brittle to plastic. Constr Build Mater 24:1–10. https://doi.org/10.1016/j.conbuildmat.2009.08.023
49. Ardanuy M, Claramunt J, Toledo Filho RD (2015) Cellulosic fiber reinforced cement-based composites: a review of recent research. Constr Build Mater 79:115–128. https://doi.org/10.1016/j.conbuildmat.2015.01.035